УНИВЕРЗИТЕТ У БЕОГРАДУ
ИНСТИТУТ ЗА ФИЗИКУ | БЕОГРАД
ИНСТИТУТ ОД НАЦИОНАЛНОГ ЗНАЧАЈА ЗА РЕПУБЛИКУ СРБИЈУ

Utilizing high-$p_\perp$ theory and data to constrain the initial stages

Bojana Ilic (Blagojevic)
Institute of Physics Belgrade
University of Belgrade

Assessing the features of Initial Stages (IS)

- Traditionally, rare high-p⊥ probes ($p_\perp \geq 5$ GeV) are utilized for studying the nature of jet-medium interactions.
- Commonly, low-p⊥ sector ($p_\perp \leq 5$ GeV) is used to infer the features of initial stages before the QGP thermalization

F. Gelis and B. Schenke, ARNPS 66, 73 (2016)

G. Aad et al. [ATLAS Collaboration], JHEP 1311, 183 (2013)

H. Niemi, G. S. Denicol, H. Holopainen and P. Huovinen, PRC 87, 054901 (2013)

- IS properties poorly-known up-to-date

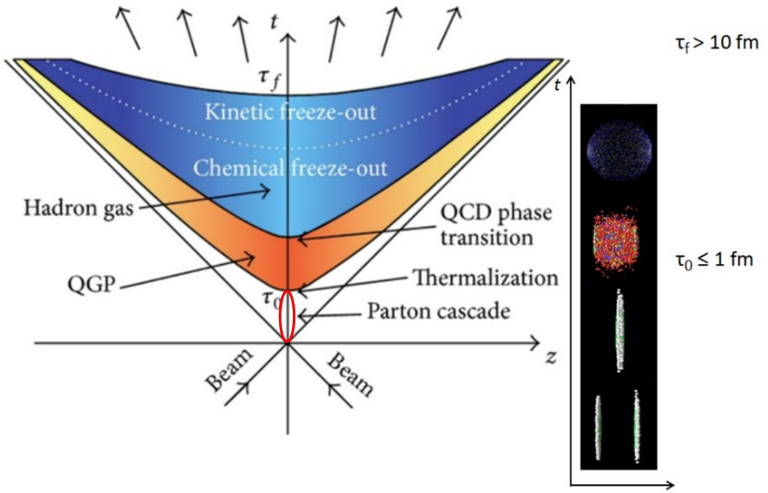

D. Zigic, B. Ilic, M. Djordjevic and M. Djordjevic, Phys. Rev. C 101, 064909 (2020)

High-$p_\perp$ observables as a novel tool for IS studies

- **High $p_\perp$ partons effectively probe** QGP properties, which in turn depend on initial QGP states
- **Recently a wealth of high-$p_\perp$ experimental data became available**

JHEP 1811, 013; JHEP 1704, 039; ATLAS-CONF-2017-012; JHEP 1807, 103; PLB 776, 195; EPJC 78, 997.

IJMPCS 46, 1860018; NPPP 289–290, 249; PRL 120, 102301; PRL 120, 202301.

NPPP 289–290, 229.

- **Current theoretical studies on this subject are either inconclusive or questionable –** e.g. the energy loss parameters were fitted to reproduce experimental R_{AA} data, individually for different analyzed T profiles.

J. Xu, A. Buzzatti and M. Gyulassy, JHEP 1408, 063 (2014)

C. Andres, N. Armesto, H. Niemi, R. Paatelainen and C. A. Salgado, PLB 803, 135318 (2020)

R. Katz, C. A. G. Prado, J. Noronha-Hostler, J. Noronha and A. A. P. Suaide, PRC 102, 024906 (2020)

D. Zigic, B. Ilic, M. Djordjevic and M. Djordjevic, Phys. Rev. C 101, 064909 (2020)

Our approach: DREENA-B

✓ For higher control over the energy loss and IS we apply full-fledged DREENA-B (Dynamical Radiative and Elastic ENergy loss Approach + Bjorken expansion) framework, because:

D. Zigic, I. Salom, M. Djordjevic and M. Djordjevic, PLB 791, 236 (2019)

❑ Dynamical energy loss formalism:
- Complex, enclosing some unique realistic features
- Dominant ingredient for generating high-$p_\perp$ predictions

M. Djordjevic and M. Djordjevic, PLB 734, 286 (2014)

❑ 1D Bjorken: J. D. Bjorken, PRD 27, 140 (1983)
- Allows analytical introduction of different evolutions before, and the same evolution after thermalization
- Facilitates isolating IS effects alone
- Presents a reasonable description of medium evolution (compared to 3+1D hydrodynamical evolution, DREENA-A)

E. Molnar, H. Holopainen, P. Huovinen and H. Niemi, PRC 90, 044904 (2014)

D. Zigic, B. Ilic, M. Djordjevic and M. Djordjevic, Phys. Rev. C 101, 064909 (2020)

Dynamical energy loss formalism

- **Finite T, finite size medium consisting of dynamical partons**
- **Based on finite T Field Theory and generalized HTL approach**

M. Djordjevic, PRC 74, 064907 (2006); PRC 80, 064909 (2009), M. Djordjevic and U. Heinz, PRL 101, 022302 (2008)

- **Collisional + radiative energy losses computed within the same theoretical framework**
- **Finite magnetic mass effect**

M. Djordjevic and M. Djordjevic, PLB 709, 229 (2012)

- **Running coupling**

M. Djordjevic and M. Djordjevic, PLB 734, 286 (2014)

- **Relaxed soft-gluon approximation**

B. Blagojevic, M. Djordjevic and M. Djordjevic, PRC 99, 024901, (2019)

All ingredients are necessary in order to accurately reproduce high-$p_\perp$ R_{AA} data!

B.Blagojevic and M. Djordjevic, JPG 42, 075105 (2015) (highlighted in LabTalk)

DREENA-B: Comparison with experimental data

D. Zigic, I. Salom, M. Djordjevic and M. Djordjevic, PLB 791, 236 (2019)

- ✓ In generating all predictions we used no fitting parameter.
- ✓ We observed a very good agreement for (where data exist):
  - Both high-$p_\perp$ R_{AA} and v_2 → no v_2 puzzle PRL 116, 252301; PLB 747, 260
  - Diverse colliding systems (Pb + Pb at 2.76 TeV and 5.02 TeV; Xe + Xe at 5.44 TeV)
  - Both light and heavy flavors ($h^\pm$, D, B)
  - All available centrality ranges

D. Zigic, B. Ilic, M. Djordjevic and M. Djordjevic, Phys. Rev. C 101, 064909 (2020)

Four common cases of Initial Stages (IS)

J. Xu, A. Buzzatti and M. Gyulassy, JHEP 1408, 063 (2014)

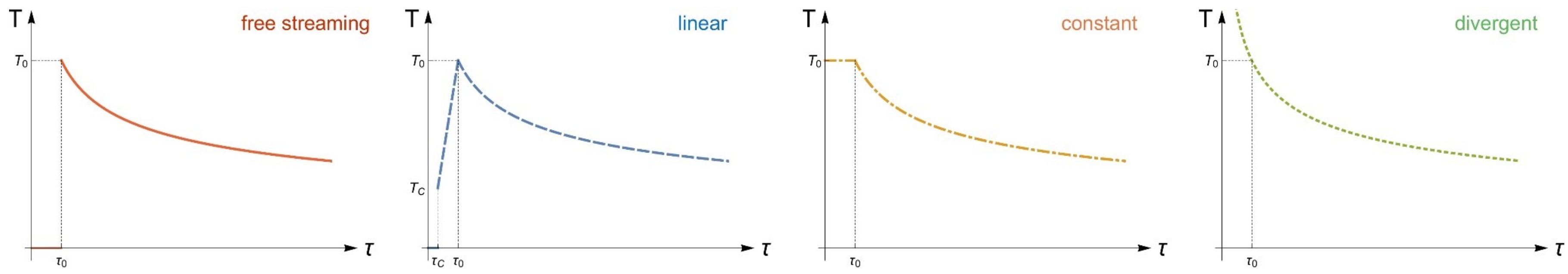

✓ Initial-stage cases have the same 1D Bjorken T profile upon thermalization, but differ for $\tau < \tau_0$=0.6 fm:

a) *Free streaming*, $T = 0$ PRD 90, 094503 (2014)

b) *Linear, linearly increasing T from T_C=160 MeV to T_0=391 MeV* (30-40 %, 5.02 TeV *Pb+Pb*)

D. Zigic, I. Salom, M. Djordjevic and M. Djordjevic, PLB 791, 236 (2019)

c) *Constant*, $T = T_0$

d) *Divergent, Bjorken expansion from the beginning ($\tau = 0$)*

D. Zigic, B. Ilic, M. Djordjevic and M. Djordjevic, Phys. Rev. C 101, 064909 (2020)

Sensitivity of high-$p_\perp$ R_{AA} to the IS

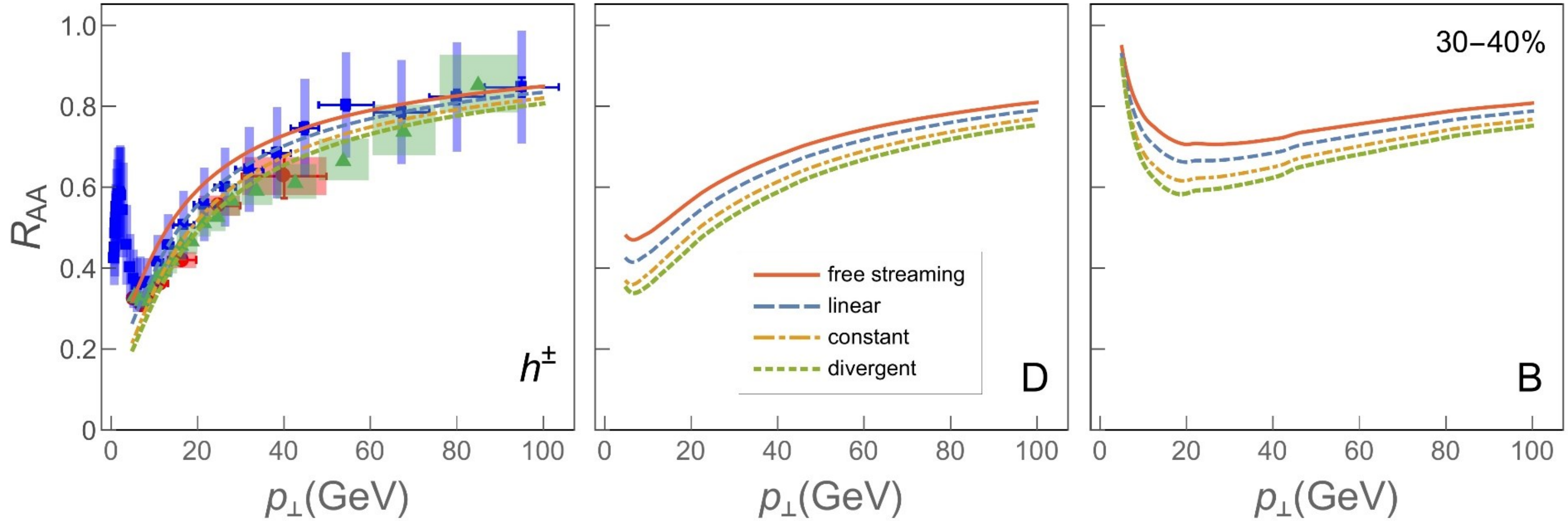

ALICE: JHEP 1811, 013 (2018);
ATLAS-CONF-2017-012;
CMS: JHEP 1704, 039 (2017)

High-$p_\perp$ R_{AA} is notably affected by the presumed initial stages, due to difference in energy loss.

However, current error-bars at the LHC do not allow distinguishing between these cases.

D. Zigic, B. Ilic, M. Djordjevic and M. Djordjevic, Phys. Rev. C 101, 064909 (2020)

Sensitivity of high-$p_\perp$ v_2 to the IS

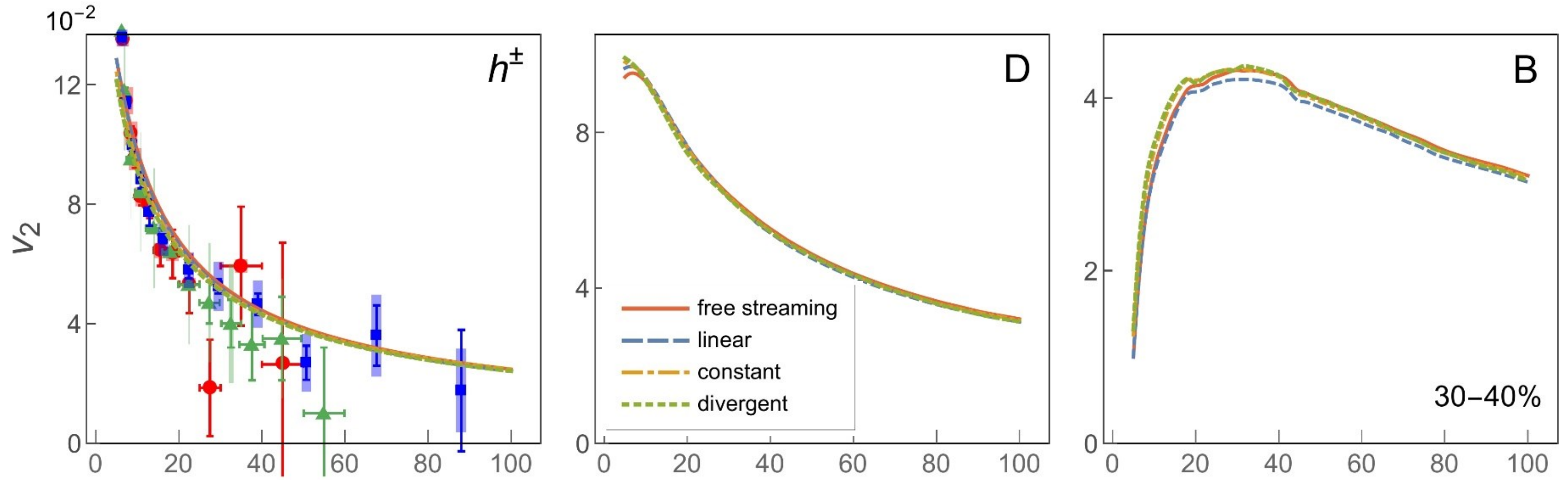

ALICE: JHEP 1807, 103 (2018);
ATLAS: EPJC 78, 997 (2018);
CMS: PLB 776, 195 (2018).

v_2 is practically insensitive to the initial stages.

C. Andres, N. Armesto, H. Niemi, R. Paatelainen and C. A. Salgado, PLB 803, 135318 (2020)

High-$p_\perp$ v_2 is unable to differentiate between different IS scenarios!

D. Zigic, B. Ilic, M. Djordjevic and M. Djordjevic, Phys. Rev. C 101, 064909 (2020)

Explanation of the obtained results

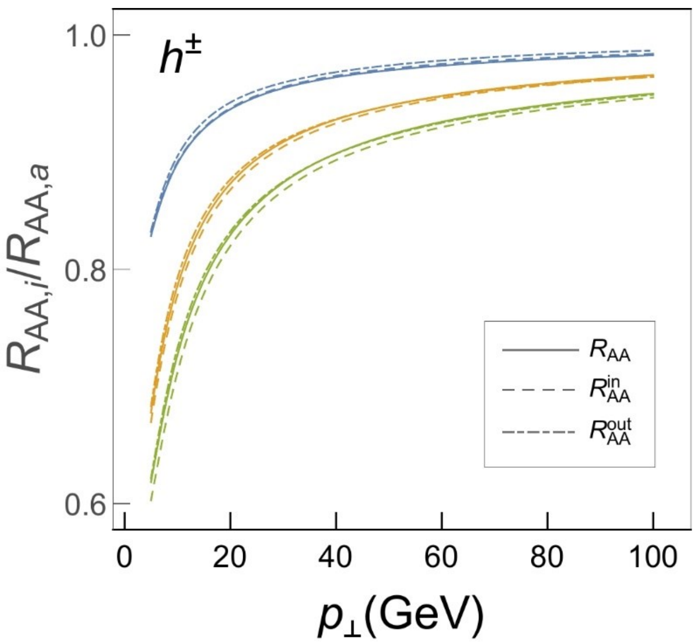

$$R_{AA} \approx \frac{R_{AA}^{in} + R_{AA}^{out}}{2}$$

$$v_2 \approx \frac{1}{2}\frac{R_{AA}^{in} - R_{AA}^{out}}{R_{AA}^{in} + R_{AA}^{out}}$$

JHEP 1408, 063

- Blue = *Linear*/*Free streaming*
- Orange = *Constant*/*Free streaming*
- Green = *Divergent*/*Free streaming*

Sets of curves

$i = lin, const, div$

Proportionality functions:

$$\gamma_i = \frac{R_{AA,i}}{R_{AA,fs}} \qquad \gamma_i^{in} = \frac{R_{AA,i}^{in}}{R_{AA,fs}^{in}} \qquad \gamma_i^{out} = \frac{R_{AA,i}^{out}}{R_{AA,fs}^{out}}$$

$$\gamma_i^{in} \approx \gamma_i^{out} \approx \gamma_i$$

$$\forall i \in \{Blue, Orange, Green\}$$

$$\gamma_i < 1$$

$$R_{AA,i} \approx \frac{\gamma_i (R_{AA,fs}^{in} + R_{AA,fs}^{out})}{2} = \gamma_i R_{AA,fs}$$

$$v_{2,i} \approx \frac{1}{2}\frac{\gamma_i (R_{AA,fs}^{in} - R_{AA,fs}^{out})}{\gamma_i (R_{AA,fs}^{in} + R_{AA,fs}^{out})} = v_{2,fs}$$

Explanation of R_{AA} results through analytical estimate

R_{AA} is shown to be sensitive only to the averaged properties of the evolving medium

$$1 - R_{AA} \sim \frac{\Delta E}{E} \sim \overline{T}$$

Analytical estimate, but for all predictions we apply full-fledged numerical calculations!

D. Zigic, I. Salom, M. Djordjevic and M. Djordjevic, PLB 791, 236 (2019)

T. Renk, PRC 85, 044903 (2012)

D. Molnar and D. Sun, NPA 932, 140 (2014); 910-911, 486 (2013)

Different $\overline{T}$s for four IS cases result in different R_{AA}s.

What are the effects of modified T-profile cases, which ensure the same average T?

D. Zigic, B. Ilic, M. Djordjevic and M. Djordjevic, Phys. Rev. C 101, 064909 (2020)

Modified temperature profiles

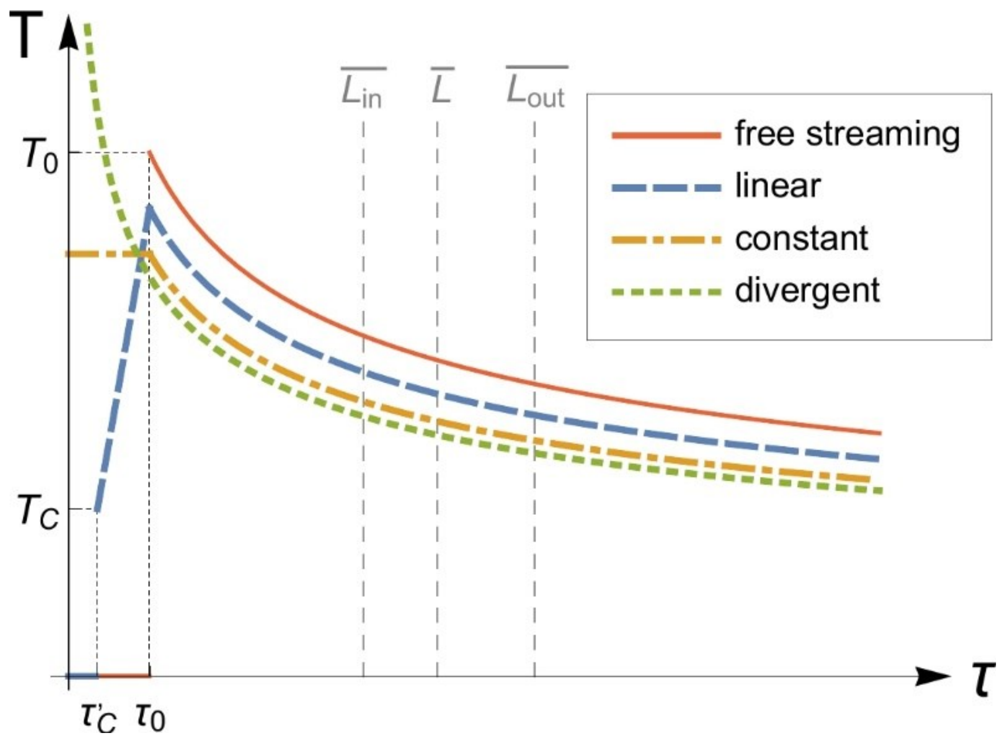

Modified T-profile cases differ not only at initial stages, but represent different evolutions altogether!

D. Zigic, B. Ilic, M. Djordjevic and M. Djordjevic, Phys. Rev. C 101, 064909 (2020)

Sensitivity of high-$p_\perp$ v_2 to modified T profiles

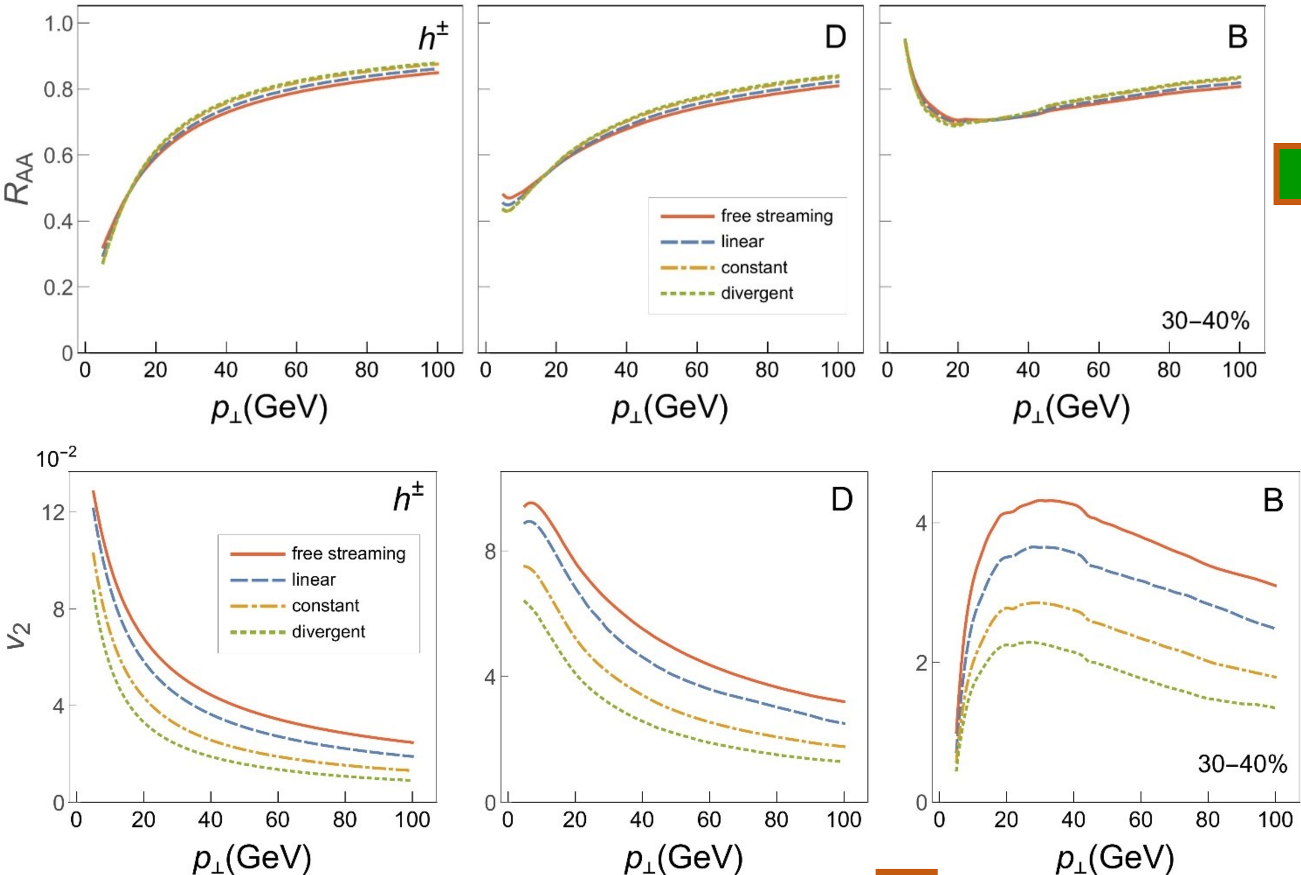

The overlap of high-$p_\perp$ R_{AA} curves in all four modified cases is verified.

High-$p_\perp$ v_2 is very sensitive to different evolutions.

The highest v_2 is observed in free-streaming case.

D. Zigic, B. Ilic, M. Djordjevic and M. Djordjevic, Phys. Rev. C 101, 064909 (2020)

Sensitivity of high-$p_\perp$ v_2 to modified T profiles

v_2 is very sensitive to these different evolutions.

Why is v_2 affected by these modified T-profile cases?

Are the initial stages at the origin of these v_2 discrepancies?

D. Zigic, B. Ilic, M. Djordjevic and M. Djordjevic, Phys. Rev. C 101, 064909 (2020)

Why is high-$p_\perp$ v_2 affected by modified T profiles?

J. Xu, A. Buzzatti, and M. Gyulassy, JHEP 1408, 063 (2014)

$$v_2 \approx \frac{1}{2}\frac{R_{AA}^{in} - R_{AA}^{out}}{R_{AA}^{in} + R_{AA}^{out}}$$

+

R_{AA} practically unchanged.

$$v_2 \sim R_{AA}^{in} - R_{AA}^{out}$$

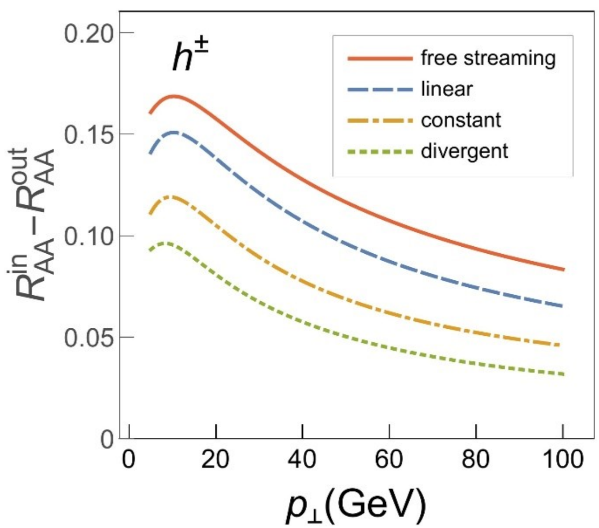

The same curve ordering as for high-$p_\perp$ v_2.

$R_{AA}^{in} - R_{AA}^{out}$ differences are responsible for high-$p_\perp$ v_2 discrepancies.

D. Zigic, B. Ilic, M. Djordjevic and M. Djordjevic, Phys. Rev. C 101, 064909 (2020)

Is IS responsible for high-p⊥ v_2 discrepancies?

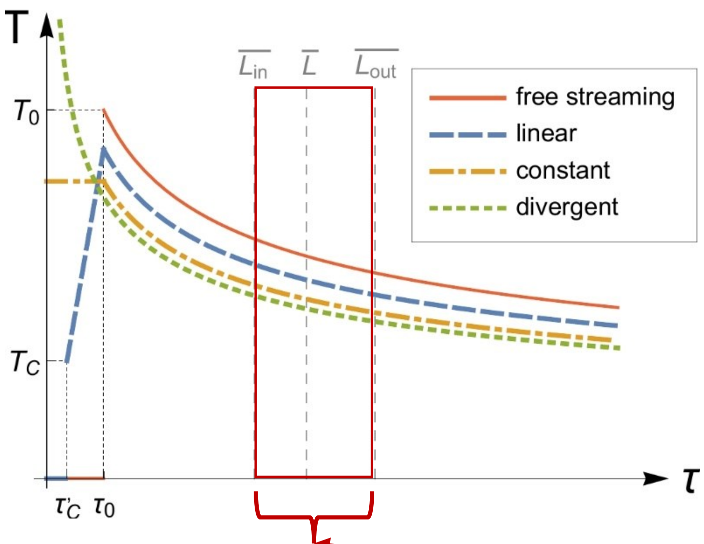

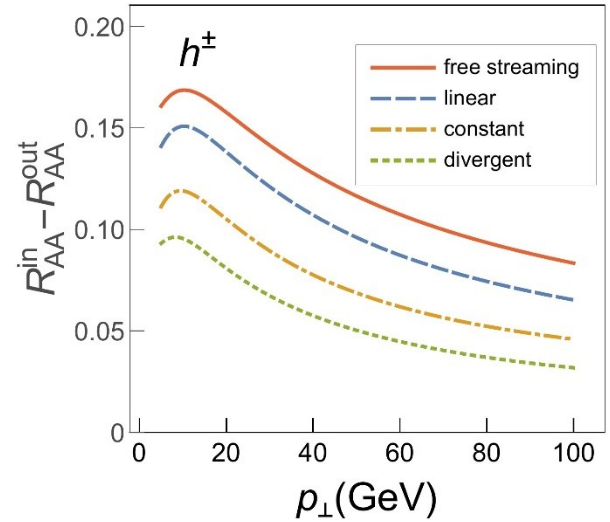

This region contributes to $R_{AA}^{in} - R_{AA}^{out}$ differences.

Large v_2 sensitivity originates from interactions of high-p⊥ parton with *thermalized* QGP, and *not the initial stages*!

D. Zigic, B. Ilic, M. Djordjevic and M. Djordjevic, Phys. Rev. C 101, 064909 (2020)

Fitting energy loss parameters to high-p⊥ R_{AA} experimental data

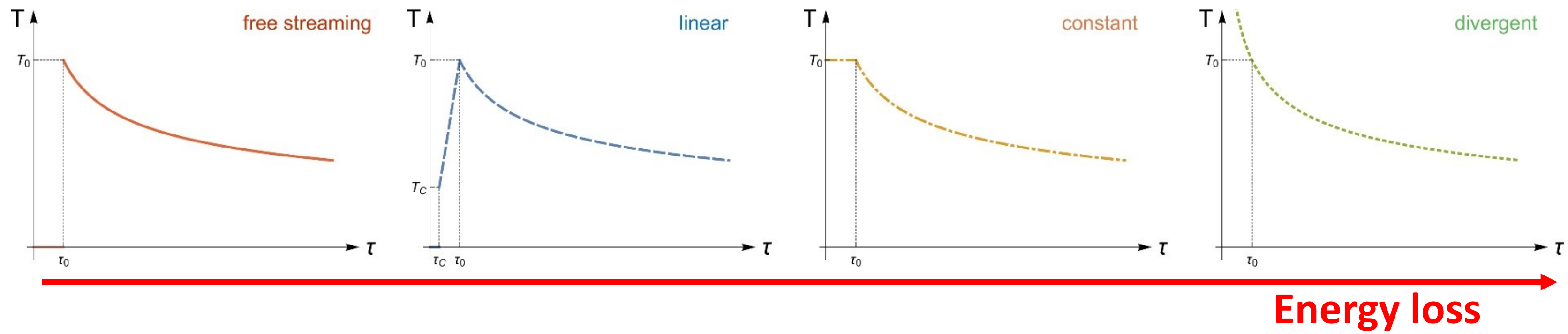

JHEP 1408, 090 (2014), PRL 116, 252301 (2016), PLB 803, 135318 (2020), PRC 96, 064903 (2017), PRC 95, 044901 (2017), PRC 96, 024909 (2017)

Fitting the energy loss (multiplicative fitting factor), to reproduce the high-p⊥ R_{AA} data, individually for different initial stages

An additional fitting factor $C_i^{fit}(p_\perp)$ is introduced in our full-fledged calculations.

Best fits to $R_{AA,fs}$ yield:

T profile case	C_i^{fit}
Free-streaming case (a)	1
Linear case (b)	0.87
Constant case (c)	0.74
Divergent case (d)	0.67

TABLE I: Fitting factors values

Sensitivity of fitted high-$p_\perp$ R_{AA} to IS

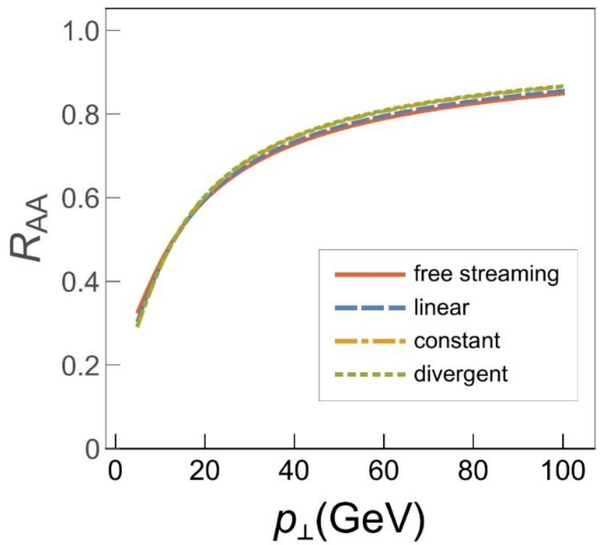

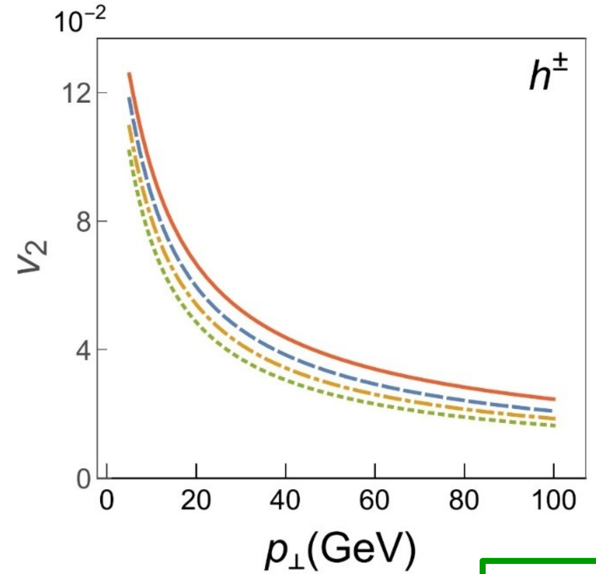

High-$p_\perp$ v_2 is notably affected!

Is this a consequence of initial stages?

High-$p_\perp$ R_{AA}s are overlapping.

C. Andres, N. Armesto, H. Niemi, R. Paatelainen and C. A. Salgado, PLB 803, 135318 (2020)

Inconsistent with our previous analysis and also intuitive expectations that higher energy loss at IS leads to lower R_{AA}!

Asymptotic scaling behavior

- **For quantitative explanation of the obtained results**
- **Assumptions:**
  - **Highly energetic jets**
  - **More peripheral collisions**

$$R_{AA} \approx 1 - \xi \overline{T}^{m} \overline{L}^{n}$$

$m \approx 1.2$

$n \approx 1.4$

S. Stojku, B. Ilic, M. Djordjevic, M. Djordjevic arXiv:2007.07851

M. Djordjevic, D. Zigic, M. Djordjevic, J. Auvinen, PRC 99, 061902 (2019)

PLB 791, 236 (2019), JPG 46, 085101 (2019)

$i = lin, const, div$

$$R^{fit}_{AA,i} \approx 1 - C_i(p_\perp)\xi \overline{T}_i^{m} \overline{L}_i^{n}$$

$$R^{fit}_{AA,i} = R_{AA,fs}$$

$$v^{fit}_{2,i} = C_i \gamma_i v_{2,fs}$$

$C_i, \gamma_i < 1$

γ_i approaches 1 at very high $p_\perp$

Differences of fitted $v_{2,i}$ compared to the *fs* case is predominantly a consequence of a decrease in the artificially imposed fitting factor.

Fitting energy loss to individual IS may result in misinterpreting the underlying physics!

PLB 803, 135318 (2020)

Conclusions

Low-$p_\perp$ sector is traditionally used to study the initial stages (IS) before QGP thermalization, but recent acquisition of wealth of high-$p_\perp$ experimental data motivated exploiting high-$p_\perp$ energy loss in studying the IS.

To this end, we utilized state-of-the-art dynamical energy loss formalism embedded in 1D Bjorken medium expansion: DREENA-B framework, to assess the effects of four commonly considered IS cases on high-$p_\perp$ observables, and obtained that high-$p_\perp$ R_{AA} is sensitive to the presumed IS. However, within the current error bars, the sensitivity is insufficient to distinguish between different initial scenarios.

Unexpectedly, we found that high-$p_\perp$ v_2 is insensitive to the IS. Moreover, by combining full-fledged numerical predictions and analytical estimates, we inferred that previously reported sensitivity of high-$p_\perp$ v_2 to IS is mostly an artefact of the fitting procedure.

Multiple fitting procedure of energy loss parameter for each individual IS may result in incorrect energy loss estimates and in overlooking the underlying physics.

Overall, the simultaneous study of high-$p_\perp$ R_{AA} and v_2, with consistent/fixed energy loss parameters across the entire study, and controlled temperature profiles, is crucial for imposing accurate constraints on the initial stages.

European Research Council
Established by the European Commission

МИНИСТАРСТВО ПРОСВЕТЕ,
НАУКЕ И ТЕХНОЛОШКОГ РАЗВОЈА

Thank you for your attention!

In collaboration with: Magdalena Djordjevic, Marko Djordjevic, Pasi Huovinen, Jussi Auvinen, Igor Salom, Dusan Zigic and Stefan Stojku

Backup

Computational scheme for jet suppression

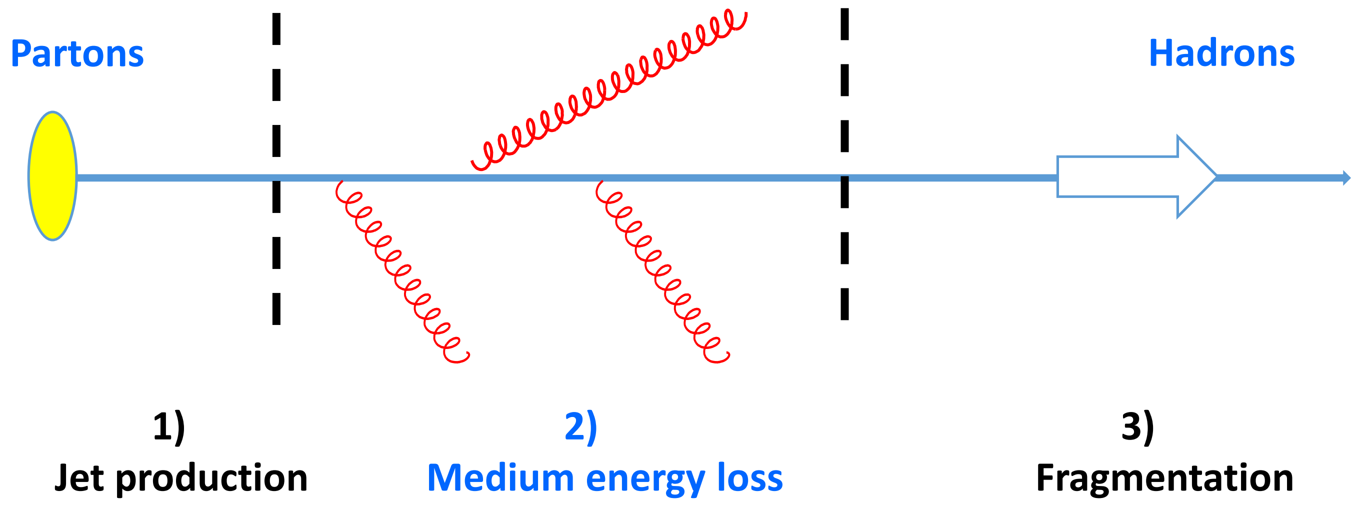

1) Initial momentum distributions
2) Energy loss calculation
3) Fragmentation function

Computational framework

$$\frac{E_f d^3\sigma}{dp_f^3} = \frac{E_i d^3\sigma(Q)}{dp_i^3} \otimes P(E_i \to E_f) \otimes D(Q \to H_Q)$$

- **Light and heavy flavor production**
  Z.B. Kang, I. Vitev, H. Xing, PLB 718:482 (2012); R. Sharma, I. Vitev, and B. W. Zhang, PRC 80, 054902 (2009)
- **Dynamical energy loss in a finite size QCD medium**
  M. Djordjevic and M. Djordjevic, PLB 734, 286 (2014)
- **Multi-gluon fluctuations**
  M. Gyulassy, P. Levai, I. Vitev, PLB 538,282 (2002)
- **Path-length fluctuations**
  A. Dainese, EPJ C33:495 (2004); S. Wicks, W. Horowitz, M. Djordjevic and M. Gyulassy, NPA 784, 426 (2007); D. Zigic, I. Salom, J. Auvinen, M. Djordjevic and M. Djordjevic, JPG 46, 085101 (2019)
- **Fragmentation for light and heavy flavor**
  DSS: D. de Florian, R. Sassot, M. Stratmann, PRD 75:114010 (2007);
  BCFY: E. Braaten, K.-M. Cheung, S. Fleming, and T. C. Yuan, PRD 51, 4819 (1995); M. Cacciari, P. Nason, JHEP 0309: 006 (2003)
  KLP: V. G. Kartvelishvili, A. K. Likhoded, and V. A. Petrov, PLB 78, 615 (1978)

Energy losses in DREENA-B framework

Radiative part:

$$\frac{dN_{rad}}{dx d\tau} = \frac{C_2(G)C_R}{\pi}\frac{1}{x}\int \frac{d^2\mathbf{q}}{\pi}\frac{d^2\mathbf{k}}{\pi}\frac{\mu_E^2(T)-\mu_M^2(T)}{[\mathbf{q}^2+\mu_E^2(T)][\mathbf{q}^2+\mu_M^2(T)]}T\alpha_s(ET)\alpha_s(\frac{\mathbf{k}^2+\chi(T)}{x})$$
$$\times\Big[1-\cos\big(\frac{(\mathbf{k}+\mathbf{q})^2+\chi(T)}{xE^+}\tau\big)\Big]\frac{2(\mathbf{k}+\mathbf{q})}{(\mathbf{k}+\mathbf{q})^2+\chi(T)}\Big[\frac{\mathbf{k}+\mathbf{q}}{(\mathbf{k}+\mathbf{q})^2+\chi(T)}-\frac{\mathbf{k}}{\mathbf{k}^2+\chi(T)}\Big]$$

$$\chi(T) = M^2x^2+m_g^2(T)$$

Collisional part:

$$\frac{dE_{coll}}{d\tau} = \frac{2C_R}{\pi v^2}\alpha_s(ET)\alpha_s(\mu_E^2(T))\int_0^\infty n_{eq}(|\vec{\mathbf{k}}|,T)d|\vec{\mathbf{k}}|$$
$$\times\Big[\int_0^{|\vec{\mathbf{k}}|/(1+v)} d|\vec{\mathbf{q}}|\int_{-v|\vec{\mathbf{q}}|}^{v|\vec{\mathbf{q}}|}\omega d\omega + \int_{|\vec{\mathbf{k}}|/(1+v)}^{|\vec{\mathbf{q}}|_{max}} d|\vec{\mathbf{q}}|\int_{|\vec{\mathbf{q}}|-2|\vec{\mathbf{k}}|}^{v|\vec{\mathbf{q}}|}\omega d\omega\Big]$$
$$\times\Big[|\Delta_L(q,T)|^2\frac{(2|\vec{\mathbf{k}}|+\omega)^2-|\vec{\mathbf{q}}|^2}{2}+|\Delta_T(q,T)|^2\frac{(|\vec{\mathbf{q}}|^2-\omega^2)((2|\vec{\mathbf{k}}|+\omega)^2+|\vec{\mathbf{q}}|^2)}{4|\vec{\mathbf{q}}|^4}(v^2|\vec{\mathbf{q}}|^2-\omega^2)\Big]$$

$$n_{eq}(|\vec{\mathbf{k}}|,T) = \frac{N}{e^{|\vec{\mathbf{k}}|/T}-1}+\frac{N_f}{e^{|\vec{\mathbf{k}}|/T}+1}$$

$$\Delta_L^{-1}(T) = \vec{\mathbf{q}}^2+\mu_E(T)^2(1+\frac{\omega}{2|\vec{\mathbf{q}}|}\ln|\frac{\omega-|\vec{\mathbf{q}}|}{\omega+|\vec{\mathbf{q}}|}|),$$

$$\Delta_T^{-1}(T) = \omega^2-\vec{\mathbf{q}}^2-\frac{\mu_E(T)^2}{2}-\frac{(\omega^2-\vec{\mathbf{q}}^2)\mu_E(T)^2}{2\vec{\mathbf{q}}^2}(1+\frac{\omega}{2|\vec{\mathbf{q}}|}\ln|\frac{\omega-|\vec{\mathbf{q}}|}{\omega+|\vec{\mathbf{q}}|}|)$$

$$|\vec{\mathbf{q}}|_{max} = \mathrm{Min}[E,\frac{2|\vec{\mathbf{k}}|(1-|\vec{\mathbf{k}}|/E)}{1-v+2|\vec{\mathbf{k}}|/E}]$$

Static vs. dynamical radiative energy loss (theory)

$$\frac{\Delta E_{rad}}{E} = \frac{C_R \alpha_S}{\pi}\frac{L}{\lambda}\int dx \frac{d^2k}{\pi}\frac{d^2q}{\pi} v(\mathbf{q}) \left(1 - \frac{\sin\frac{(\mathbf{k}+\mathbf{q})^2+\chi}{xE^+}L}{\frac{(\mathbf{k}+\mathbf{q})^2+\chi}{xE^+}L}\right) \frac{2(\mathbf{k}+\mathbf{q})}{(\mathbf{k}+\mathbf{q})^2+\chi}\left(\frac{(\mathbf{k}+\mathbf{q})}{(\mathbf{k}+\mathbf{q})^2+\chi} - \frac{\mathbf{k}}{\mathbf{k}^2+\chi}\right)$$

Two differences:

***v*(q) effective cross section:**

$$\left[\frac{\mu^2}{(\mathbf{q}^2+\mu^2)^2}\right]_{stat} \longrightarrow \left[\frac{\mu^2}{\mathbf{q}^2(\mathbf{q}^2+\mu^2)}\right]_{dyn}$$

λ mean free path:

$$\frac{1}{\lambda_{stat}} \longrightarrow \frac{1}{\lambda_{dyn}} = \frac{1}{c(n_f)}\frac{1}{\lambda_{stat}}$$

Increases energy loss rate in dynamical medium

where: $$\frac{1}{\lambda_{dyn}} = 3\alpha_S T$$

$$c(n_f) = 6\frac{1.202}{\pi^2}\frac{1+n_f/4}{1+n_f/6}$$

Finite magnetic mass effect on R_{AA} (theory)

$$\frac{\Delta E_{rad}}{E} = \frac{C_R \alpha_S}{\pi}\frac{L}{\lambda}\int dx \frac{d^2k}{\pi}\frac{d^2q}{\pi} v(\mathbf{q}) \left(1-\frac{\sin\frac{(\mathbf{k}+\mathbf{q})^2+\chi}{xE^+}L}{\frac{(\mathbf{k}+\mathbf{q})^2+\chi}{xE^+}L}\right)\frac{2(\mathbf{k}+\mathbf{q})}{(\mathbf{k}+\mathbf{q})^2+\chi}\left(\frac{(\mathbf{k}+\mathbf{q})}{(\mathbf{k}+\mathbf{q})^2+\chi}-\frac{\mathbf{k}}{\mathbf{k}^2+\chi}\right)$$

Only this part gets modified

$$v(\mathbf{q}) = \frac{\mu_E^2}{\mathbf{q}^2(\mathbf{q}^2+\mu_E^2)} \longrightarrow \frac{\mu_E^2-\mu_M^2}{(\mathbf{q}^2+\mu_E^2)(\mathbf{q}^2+\mu_M^2)}$$

$$0.4 \leq \frac{\mu_M}{\mu_E} \leq 0.6$$

Causes suppression decrease

Yu. Maezawa et al. [WHOT-QCD Collaboration], PRD 81, 091501 (2010)
A. Nakamura, T. Saito and S. Sakai, PRD 69, 014506 (2004)
A. Hart, M. Laine and O. Philipsen, NPB 586, 443 (2000)
D. Bak, A. Karch and L. G. Yaffe, JHEP 0708, 049 (2007)

M.Djordjevic and M. Djordjevic, PLB 709:229 (2012)

Finite magnetic mass effect

$$v(\mathbf{q}) = v_L(\mathbf{q}) - v_T(\mathbf{q})$$

$$v_{L,T}(\mathbf{q}) = \frac{1}{\mathbf{q}^2 + Re\Pi_{L,T}(\infty)} - \frac{1}{\mathbf{q}^2 + Re\Pi_{L,T}(0)}$$

$$Re\Pi_T(\infty) = Re\Pi_L(\infty) \equiv \mu_{pl}^2$$

$$\mu_E^2 \equiv Re\Pi_L(x=0)$$

$$\mu_M^2 \equiv Re\Pi_T(x=0)$$

Running coupling

Collisional energy loss

S. Peigne, A. Peshier, PRD 77:14017 (2008)

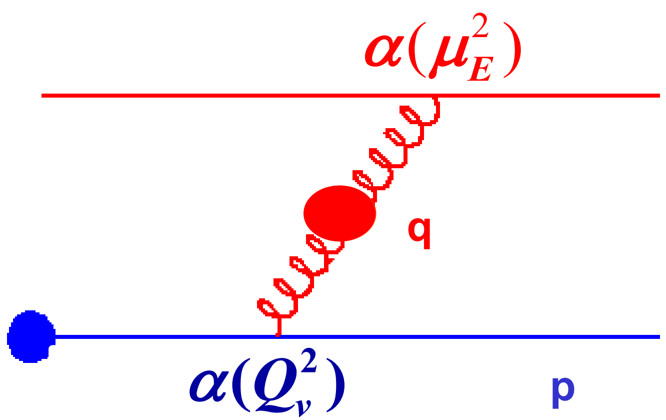

$$\Delta E_{coll} \sim \alpha(Q_v^2)\,\alpha(\mu_E^2)$$

$$\alpha_S(Q^2) = \frac{4\pi}{(11 - 2/3 n_f)\ln(Q^2/\Lambda_{QCD}^2)}$$

$$\frac{\mu_E^2}{\Lambda_{QCD}^2}\ln\left(\frac{\mu_E^2}{\Lambda_{QCD}^2}\right) = \frac{1+n_f/6}{11-2/3\,n_f}\left(\frac{4\pi T}{\Lambda_{QCD}}\right)^2$$

A. Peshier, hep-ph/0601119 (2006)

Radiative energy loss

M. D. and M. Djordjevic, PLB 734 : 286 (2014)

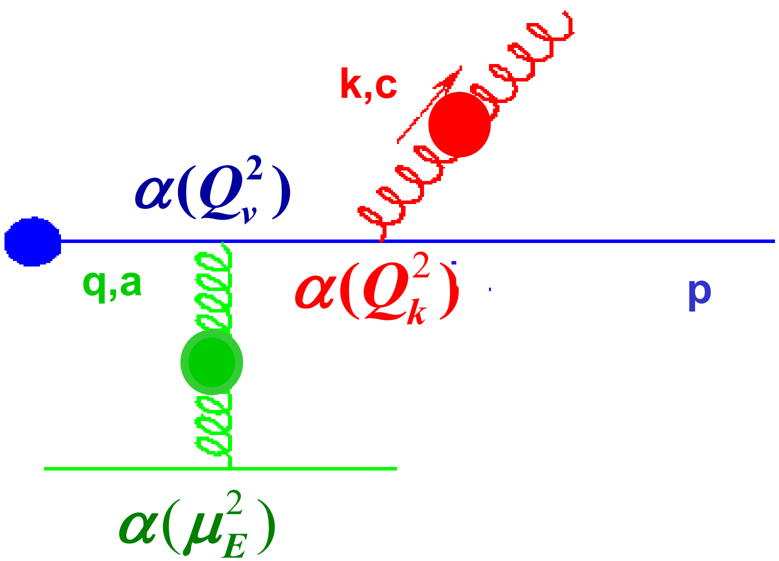

$$\Delta E_{rad} \sim \alpha(Q_k^2)\,\alpha(Q_v^2)\,\alpha(\mu_E^2)$$

$$Q_v^2 = ET$$

$$Q_k^2 = \frac{\mathbf{k}^2 + M^2 x^2 + m_g^2}{x}$$

Relaxing the soft-gluon approximation

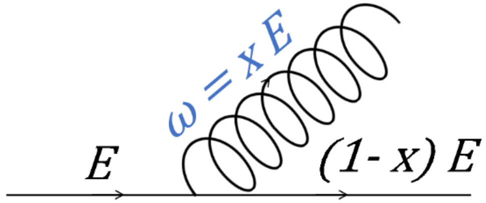

- **The soft-gluon approximation (*sg*) definition – radiated gluon carries away a small fraction of initial jet energy $x = \frac{\omega}{E} \ll 1$.**
- **Widely-used assumption in calculating radiative energy loss of high $p_\perp$ particle traversing QGP**

ASW (PRD, 69:114003), BDMPS (NPB, 484:265), BDMPS-Z (JETP Lett., 65:615), GLV (NPB 594:371), HT (NPA 696:788);

M. Djordjevic, PRC , 80:064909 (2009), M. Djorjevic and U. Heinz, PRL, 101:022302 (2008)

Calculations beyond soft-gluon approximation

0th order

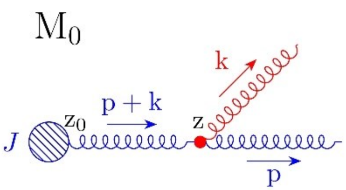

Interaction with one scatterer

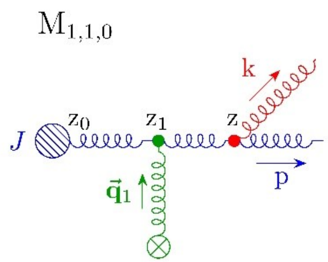

Interaction with two scatterers in contact limit

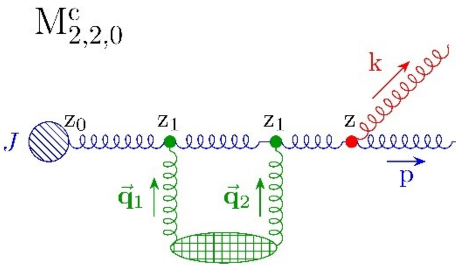

- **Beyond soft-gluon approximation (*bsg*) in DGLV:** x **finite**
- **Assumptions:**
  - **Initial gluon propagates along the longitudinal axis**
  - **The soft-rescattering (eikonal) approximation**
  - **The 1st order in opacity approximation**

(M. Gyulassy, P. Levai and I. Vitev, PLB 538:282 (2002))

(B. Blagojevic, M. Djordjevic and M. Djordjevic, PRC 99, 024901, (2019))

Comparison of analytical expressions ($\frac{dN_g^{(1)}}{dx}$)

Beyond soft-gluon approximation:

$$f_{bsg}(\boldsymbol{k},\boldsymbol{q}_1,x)=\frac{(1-x+x^2)^2}{x(1-x)}\left\{\left(2\frac{(\boldsymbol{k}-\boldsymbol{q}_1)^2}{(\boldsymbol{k}-\boldsymbol{q}_1)^2+\chi}-\frac{\boldsymbol{k}\cdot(\boldsymbol{k}-\boldsymbol{q}_1)}{\boldsymbol{k}^2+\chi}-\frac{(\boldsymbol{k}-\boldsymbol{q}_1)\cdot(\boldsymbol{k}-x\boldsymbol{q}_1)}{(\boldsymbol{k}-x\boldsymbol{q}_1)^2+\chi}\right)\frac{(\boldsymbol{k}-\boldsymbol{q}_1)^2+\chi}{\left(\frac{4x(1-x)E}{L}\right)^2+\left((\boldsymbol{k}-\boldsymbol{q}_1)^2+\chi\right)^2}\right.$$

$$\left.+\frac{\boldsymbol{k}^2+\chi}{\left(\frac{4x(1-x)E}{L}\right)^2+\left(\boldsymbol{k}^2+\chi\right)^2}\left(\frac{\boldsymbol{k}^2}{\boldsymbol{k}^2+\chi}-\frac{\boldsymbol{k}\cdot(\boldsymbol{k}-x\boldsymbol{q}_1)}{(\boldsymbol{k}-x\boldsymbol{q}_1)^2+\chi}\right)+\left(\frac{(\boldsymbol{k}-x\boldsymbol{q}_1)^2}{((\boldsymbol{k}-x\boldsymbol{q}_1)^2+\chi)^2}-\frac{\boldsymbol{k}^2}{(\boldsymbol{k}^2+\chi)^2}\right)\right\}$$

$$\chi=m_g^2(1-x+x^2)$$

Soft-gluon approximation:

$$f_{sg}(\boldsymbol{k},\boldsymbol{q}_1,x)=\frac{1}{x}\frac{(\boldsymbol{k}-\boldsymbol{q}_1)^2+m_g^2}{\left(\frac{4xE}{L}\right)^2+((\boldsymbol{k}-\boldsymbol{q}_1)^2+m_g^2)^2}2\left(\frac{(\boldsymbol{k}-\boldsymbol{q}_1)^2}{(\boldsymbol{k}-\boldsymbol{q}_1)^2+m_g^2}-\frac{\boldsymbol{k}\cdot(\boldsymbol{k}-\boldsymbol{q}_1)}{\boldsymbol{k}^2+m_g^2}\right)$$

M. Djordjevic and M. Gyulassy, NPA 733:265(2004)

Only this term remains in *sg* and reduces to:

(B. Blagojevic, M. Djordjevic and M. Djordjevic, PRC 99, 024901, (2019))

Bsg **expression is quite different and notably more complex than its *sg* analogon!**

Effect of relaxing *sga* on numerical predictions

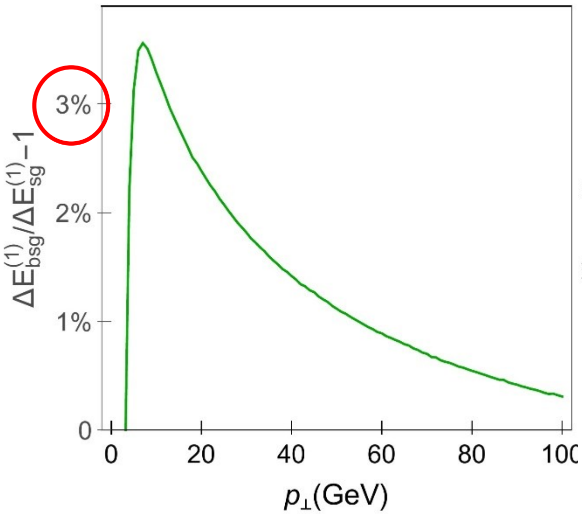

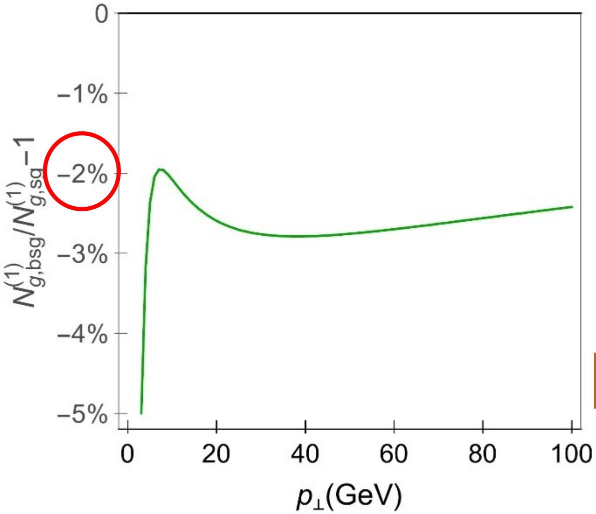

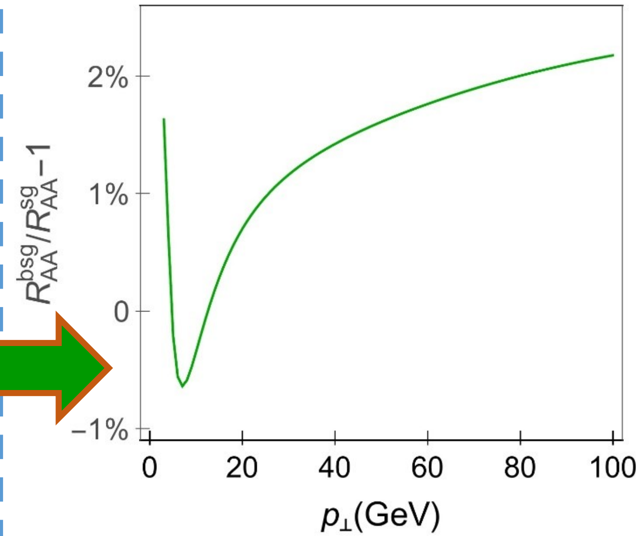

Slightly increased $\frac{\Delta E}{E}$ compared to *sg*.

Slightly decreased N_g compared to *sg*.

R_{AA} negligibly affected!

Effect on $\Delta E^{(1)}/E$ and $N_g^{(1)}$ is very small and of an opposite sign, and they both non-trivially affect R_{AA}!

Interplay of the opposite effects on $\Delta E^{(1)}/E$ and $N_g^{(1)}$ is responsible for negligible effect on R_{AA}.

(B. Blagojevic, M. Djordjevic and M. Djordjevic, PRC 99, 024901, (2019))

Multi-gluon fluctuations

M. Gyulassy, P. Levai, I. Vitev, PLB 538,282 (2002)

Poisson distribution:

$$P(k \text{ events in interval}) = \frac{\lambda^k e^{-\lambda}}{k!}$$

where

- λ is the average number of events per interval

$$\text{Poisson expansion } P(\epsilon, E) = \sum_{n=0}^{\infty} P_n(\epsilon, E)$$

$$\epsilon = \sum_i \omega_i / E$$

$$P_0(\epsilon, E) = e^{-\langle N^g(E) \rangle} \delta(\epsilon)$$

$$P_1(\epsilon, E) = e^{-\langle N^g \rangle} \rho(\epsilon, E)$$

$$\rho(x) = dN_g/dx = \sum_{n=1}^{\infty} \rho^{(n)}(x)$$

$$P_{n+1}(\epsilon, E) = \frac{1}{n+1} \int_{x_0}^{1-x_0} dx_n \, \rho(x_n, E) P_n(\epsilon - x_n, E)$$

$$= \frac{e^{-\langle N^g(E) \rangle}}{(n+1)!} \int dx_1 \cdots dx_n \, \rho(x_1, E) \cdots \rho(x_n, E) \rho(\epsilon - x_1 - \cdots - x_n, E)$$

$$\int_0^{\infty} d\epsilon \, P(\epsilon, E) \epsilon = \frac{\Delta E}{E}$$

$$m_g = m_\infty = \sqrt{\Pi_T(p_0/|\vec{\mathrm{p}}| = 1)} = \mu_E/\sqrt{2}$$

Effective gluon mass

M. Djordjevic and M. Gyulassy, PRC 68:034914 (2003)

$$\Delta E/E \approx \chi \overline{T}^m \overline{L}^n,$$

$$R_{AA} \approx 1 - \frac{l-2}{2}\frac{\Delta E}{E} = 1 - \xi \overline{T}^m \overline{L}^n$$

M. Gyulassy, P. Levai and I. Vitev, PLB 538, 282 (2002)

$$R^{fit}_{AA,i} \approx 1 - C_i \xi \overline{T}^m_i \overline{L}^n_i \approx 1 - C_i(1 - R_{AA,i})$$

$$C_i \approx \frac{1 - R^{fit}_{AA,i}}{1 - R_{AA,i}}$$

$$C_i \approx \frac{v^{fit}_{2,i}}{\gamma_{ia} v_{2,a}}$$

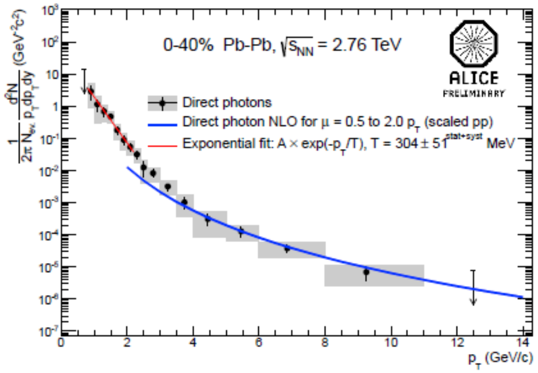

ALICE: NPA 904-905 573c (2013)

(T_{eff}) of 304 MeV for 0-40% centrality 2.76 TeV Pb+Pb

$$T^3 \sim \frac{\frac{dN_g}{dy}}{A_\perp \overline{L}} \to T = c\left(\frac{\frac{dN_ch}{dy}}{A_\perp \overline{L}}\right)^{1/3}$$

average medium temperature of 348 MeV in most central 5.02 TeV Pb+Pb

M. Gyulassy, P. Levai and I. Vitev, NPB 594 371 (2001);
J. Xu, A. Buzzatti and M. Gyulassy, JHEP 1408, 063 (2014)

M. Djordjevic, M. Djordjevic and B. Blagojevic, PLB 737, 298 (2014)

+

$T_C \approx$ 150 MeV

PRD 90, 094503 (2014)

M. Djordjevic, M. Gyulassy, R. Vogt and S. Wicks, PLB 632, 81 (2006)

$T_0 \sim (dN_{ch}/dy/A_\perp)^{1/3}$

$T_0 = 500$ MeV in most central 5.02 TeV Pb+Pb

For each centrality region.

J. Xu, A. Buzzatti, and M. Gyulassy, JHEP 1408, 063 (2014)
P. Christiansen, K. Tywoniuk and V. Vislavicius, PRC 89, 034912 (2014)

$$\begin{cases} R_{AA}^{\text{in}}(p_T) \approx \dfrac{\frac{dN_h^{AA}}{dydp_T}(1+2v_2+2v_4\cdots)}{N_{\text{binary}}\frac{dN_h^{pp}}{dydp_T}} = R_{AA}^h\,(1+2v_2+2v_4\cdots) \\ R_{AA}^{\text{out}}(p_T) = \dfrac{\frac{dN_h^{AA}}{dydp_T}(1-2v_2-2v_4\cdots)}{N_{\text{binary}}\frac{dN_h^{pp}}{dydp_T}} = R_{AA}^h\,(1-2v_2-2v_4\cdots) \end{cases}$$

$$v_2 \approx \frac{1}{2}\frac{R_{AA}^{in} - R_{AA}^{out}}{R_{AA}^{in} + R_{AA}^{out}}$$

$$\frac{\mathrm{d}N}{\mathrm{d}\varphi} \propto 1 + 2\sum_{n=1}^{+\infty} v_n \cos[n(\varphi - \Psi_n)]$$

EbyE effect on v_2

J. Noronha-Hostler, B. Betz, J. Noronha, and M. Gyulassy, PRL 116, 252301 (2016);
S. Shi, J. Liao, and M. Gyulassy, CPC 42, 104104 (2018); 43, 044101 (2019)
S. Cao, L. G. Pang, T. Luo, Y. He, G. Y. Qin, and X. N. Wang, NPPP 289–290, 217 (2017)

Modified T profiles

T profile case	T_0' (MeV)
Free-streaming case (a)	391
Modified linear case (b')	$391 \times (1 - 10.7\%)$
Modified constant case (c')	$391 \times (1 - 19.3\%)$
Modified divergent case (d')	$391 \times (1 - 23.7\%)$

TABLE I: Initial temperatures for modified T profiles

Verification of analytic estimate

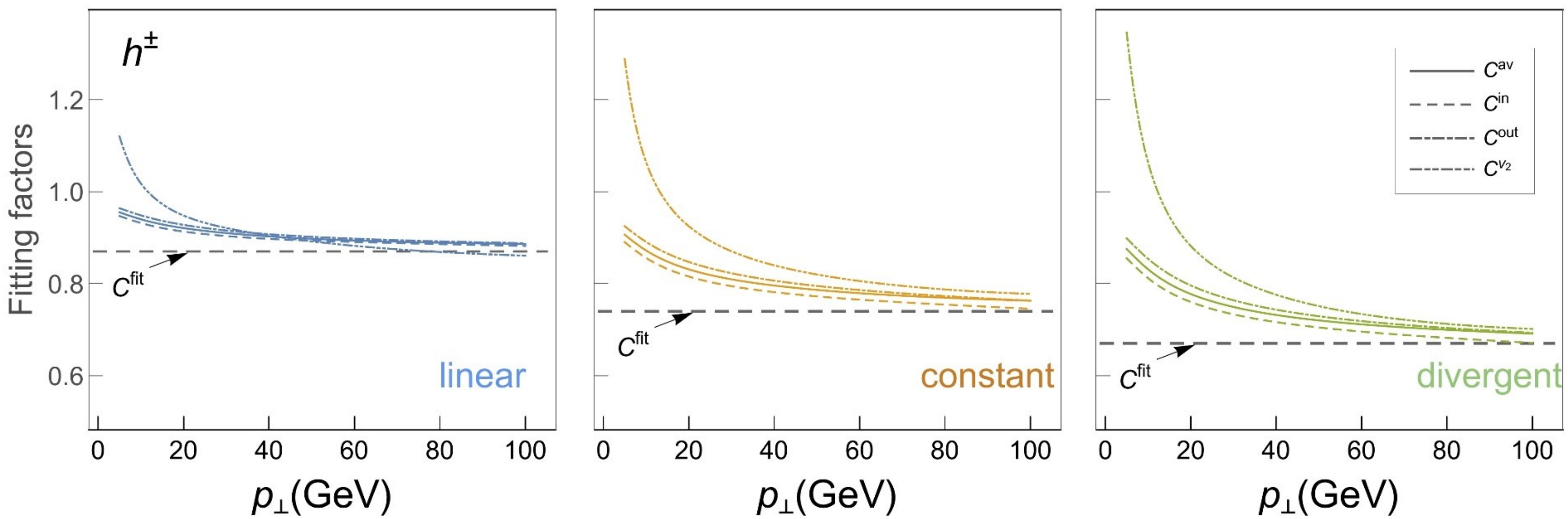

$$C_i^{in} = \frac{1 - R_{AA,i}^{in,fit}}{1 - R_{AA,i}^{in}}, \quad C_i^{out} = \frac{1 - R_{AA,i}^{out,fit}}{1 - R_{AA,i}^{out}},$$

$$C_i^{av} = \frac{1 - R_{AA,i}^{fit}}{1 - R_{AA,i}}, \quad C_i^{v_2} = \frac{1}{\gamma_i} \frac{v_{2,i}^{fit}}{v_{2,a}},$$

$$C_i \approx \frac{v_{2,i}^{\text{fit}}}{\gamma_{ia} v_{2,a}}$$

D. Zigic, B. Ilic, M. Djordjevic and M. Djordjevic, Phys. Rev. C 101, 064909 (2020)

- Models that explain both **high-$p_\perp$ R_{AA}** and **v_2** data assume **the same** starting time of jet quenching and the hydrodynamic expansion (more precisely common assumption is free streaming of high-$p_\perp$ particles at IS in energy loss models and non-existing pre-equilibrium evolution in hydrodynamical simulations).

S. Stojku, J. Auvinen, M. Djordjevic, P. Huovinen, M. Djordjevic, arXiv:2008.08987 (2020)

D. Zigic, I. Salom, J. Auvinen, M. Djordjevic, M. Djordjevic, PLB 791, 236 (2019)

J. Noronha-Hostler, B. Betz, J. Noronha, M. Gyulassy, PRL 116, 252301 (2016)

S. Shi, J. Liao, M. Gyulassy, Chin. Phys. C 42, 104104 (2018)

S. Shi, J. Liao, M. Gyulassy, Chin. Phys. C 43, 044101 (2019)

W. van der Schee, P. Romatschke and S. Pratt, PRL 111, 222302 (2013)
J. Liu, C. Shen and U. Heinz, PRC 91, 064906 (2015)
B. Schenke, C. Shen and P. Tribedy, PLB 803, 135322 (2020)
T. Nunes da Silva, D. Chinellato, M. Hippert, W. Serenone, J. Takahashi, G. S. Denicol, M. Luzum and J. Noronha, arXiv:2006.02324

Dainese [ALICE Collaboration], EPJC 33, 495 (2004);
D. Zigic, I. Salom, J. Auvinen, M. Djordjevic and M. Djordjevic, JPG 46, 085101 (2019)

$$L(x,y,\phi) = \frac{\int_0^\infty \mathrm{d}\lambda\, \lambda\, \rho(x+\lambda\cos(\phi), y+\lambda\sin(\phi))}{\int_0^\infty \mathrm{d}\lambda\, \rho(x+\lambda\cos(\phi), y+\lambda\sin(\phi))}$$

ρ initial density distribution of QGP droplet

S. Afanasiev et al. [PHENIX Collaboration], PRC 80, 054907 (2009)

$$\langle L_{in}\rangle = \frac{1}{\Delta\phi}\int_{-\Delta\phi/2}^{\Delta\phi/2} \mathrm{d}\phi\, \langle L(\phi)\rangle$$

$$\langle L_{out}\rangle = \frac{1}{\Delta\phi}\int_{\pi/2-\Delta\phi/2}^{\pi/2+\Delta\phi/2} \mathrm{d}\phi\, \langle L(\phi)\rangle$$

Constraining bulk QGP properties with high-pT observables

$$\frac{v_2}{1-R_{AA}} \approx \frac{1}{2}\left(b-\frac{a}{c}\right)\frac{\langle L_{out}\rangle - \langle L_{in}\rangle}{\langle L_{out}\rangle + \langle L_{in}\rangle} \approx 0.57\varsigma,$$

$$\text{where } \varsigma = \frac{\langle L_{out}\rangle - \langle L_{in}\rangle}{\langle L_{out}\rangle + \langle L_{in}\rangle} \text{ and } \frac{1}{2}(b-\frac{a}{c}) \approx 0.57$$

$$\epsilon_{2L} = \frac{\langle L_{out}\rangle^2 - \langle L_{in}\rangle^2}{\langle L_{out}\rangle^2 + \langle L_{in}\rangle^2} = \frac{2\varsigma}{1+\varsigma^2}$$

$$\epsilon_2 = \frac{\langle y^2 - x^2\rangle}{\langle y^2 + x^2\rangle} = \frac{\int \mathrm{d}x\,\mathrm{d}y\,(y^2-x^2)\,\rho(x,y)}{\int \mathrm{d}x\,\mathrm{d}y\,(y^2+x^2)\,\rho(x,y)}$$

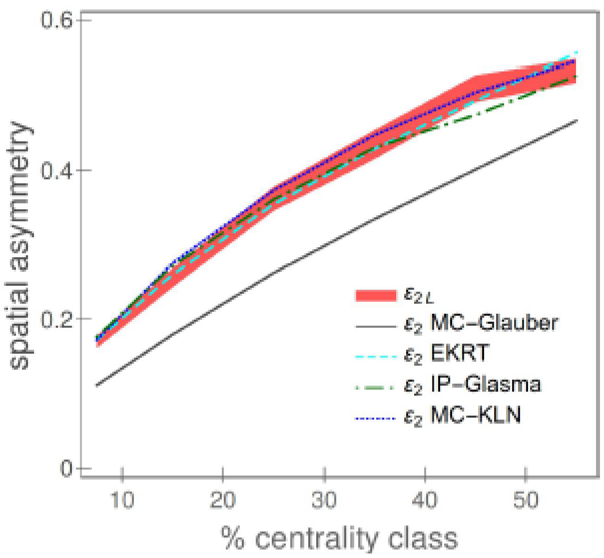

M. Djordjevic, S. Stojku, M.Djordjevic, P.Huovinen, PRC 100, 031901 (2019)

Constraining bulk QGP properties with joint low- and high-pT observables

S. Stojku, J. Auvinen, M. Djordjevic, P. Huovinen, M. Djordjevic, arXiv:2008.08987 (2020)

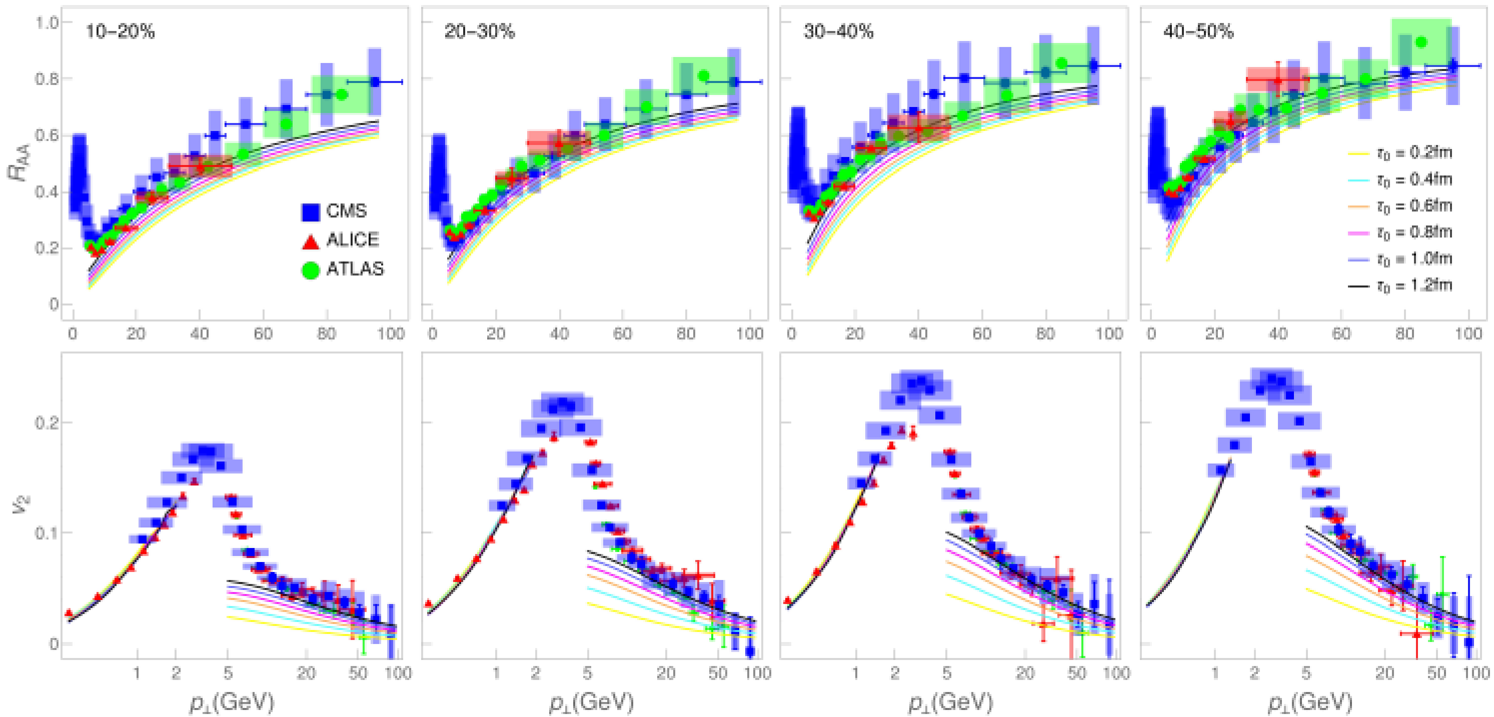

Later thermalization time is preferred (τ ~ 1fm)

PRC 90, 044904 (2014)

Radiative energy loss

Radiative energy loss comes from the processes in which there are more outgoing than incoming particles:

0^{th} order

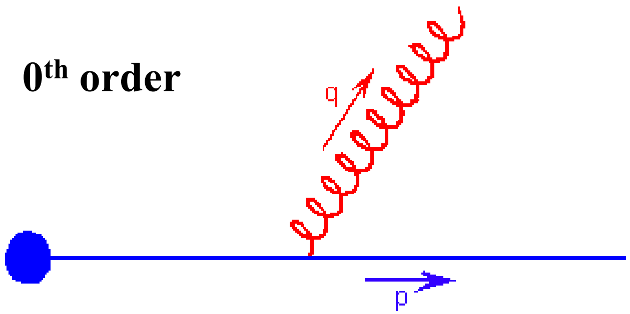

1^{st} order

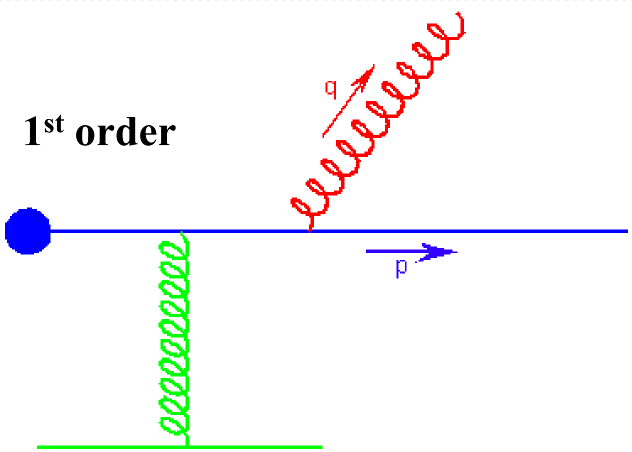

Collisional energy loss

Collisional (elastic) energy loss comes from the processes which have the same number of incoming and outgoing particles:

0^{th} order

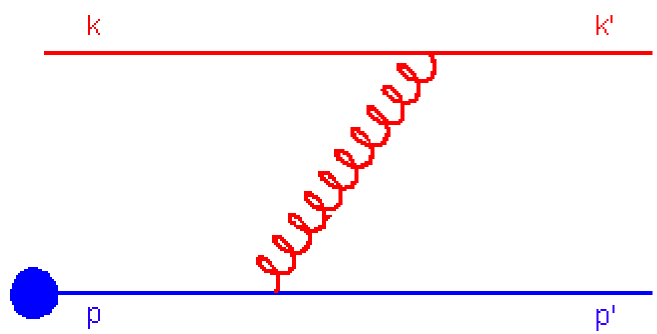

Collisional energy loss in a finite size QCD medium

Consider a medium of size L in thermal equilibrium at temperature T.

The main order collisional energy loss is determined from:

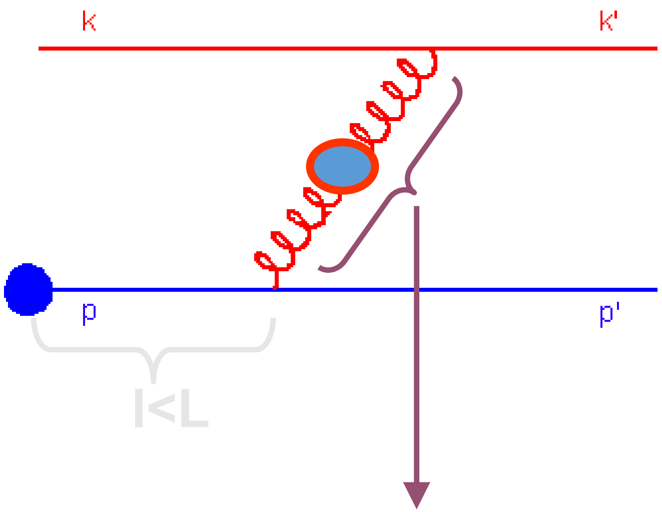

The effective gluon propagator:

$$D^{\mu\nu}(\omega, \vec{\mathrm{q}}) = -P^{\mu\nu}\Delta_T(\omega, \vec{\mathrm{q}}) - Q^{\mu\nu}\Delta_L(\omega, \vec{\mathrm{q}})$$

M. D., Phys.Rev.C74:064907,2006

Radiative energy loss in a dynamical medium

We compute the medium induced radiative energy loss for a heavy quark to first (lowest) order in number of scattering centers.

To compute this process, we consider the radiation of one gluon induced by one collisional interaction with the medium.

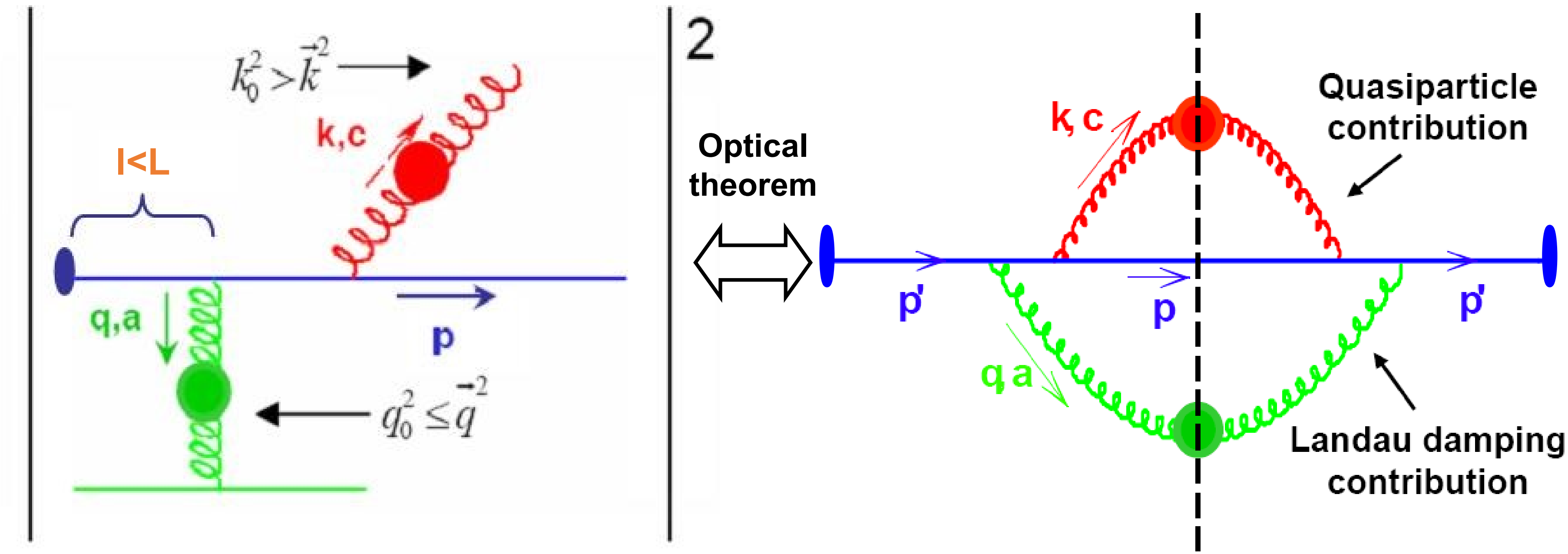

We consider a medium of finite size L, and assume that the collisional interaction has to occur inside the medium.

The calculations were performed by using two Hard-Thermal Loop approach

1-HTL gluon propagator:

$$iD^{\mu\nu}(l) = \frac{P^{\mu\nu}(l)}{l^2-\Pi_T(l)} + \frac{Q^{\mu\nu}(l)}{l^2-\Pi_L(l)}$$

Cut 1-HTL gluon propagator:

$$D^{>}_{\mu\nu}(l) = -(1+f(l_0))\Big(P_{\mu\nu}(l)\rho_T(l) + Q_{\mu\nu}(l)\rho_L(l)\Big)\ ,$$

$$\rho_{L,T}(l) = \underbrace{2\pi\,\delta(l^2-\Pi_{T,L}(l))}_{\text{Radiated gluon}} - \underbrace{2\,\mathrm{Im}\left(\frac{1}{l^2-\Pi_{T,L}(l)}\right)\theta(1-\frac{l_0^2}{\vec{l}^2})}_{\text{Exchanged gluon}}$$

For radiated gluon, cut 1-HTL gluon propagator can be simplified to

(M.D. and M. Gyulassy, PRC 68, 034914 (2003).

$$D^{>}_{\mu\nu}(k) \approx -2\pi\,\frac{P_{\mu\nu}(k)}{2\omega}\,\delta(k_0-\omega) \qquad \omega \approx \sqrt{\vec{k}^2+m_g^2}\,;\ m_g \approx \mu/\sqrt{2}$$

For exchanged gluon, cut 1-HTL gluon propagator cannot be simplified, since both transverse (magnetic) and longitudinal (electric) contributions will prove to be important.

$$D^{>}_{\mu\nu}(q) = \theta(1-\frac{q_0^2}{\vec{q}^2})\,(1+f(q_0))\,2\,\mathrm{Im}\left(\frac{P_{\mu\nu}(q)}{q^2-\Pi_T(q)} + \frac{Q_{\mu\nu}(q)}{q^2-\Pi_L(q)}\right)$$

Is IS responsible for high-p⊥ v_2 discrepancies?

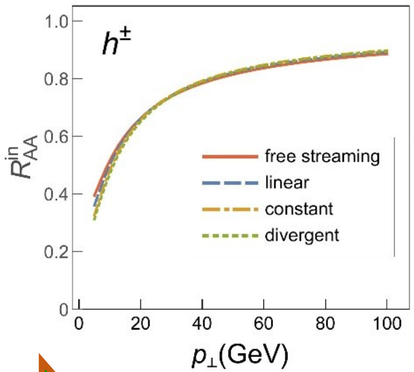

No effect on R_{AA}^{in}.

Only R_{AA}^{out} differences are responsible for v_2 discrepancies.

$-R_{AA} \sim \overline{T}$

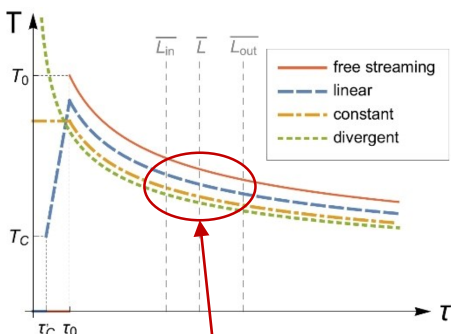

Only this region contributes to R_{AA}^{out} differences.

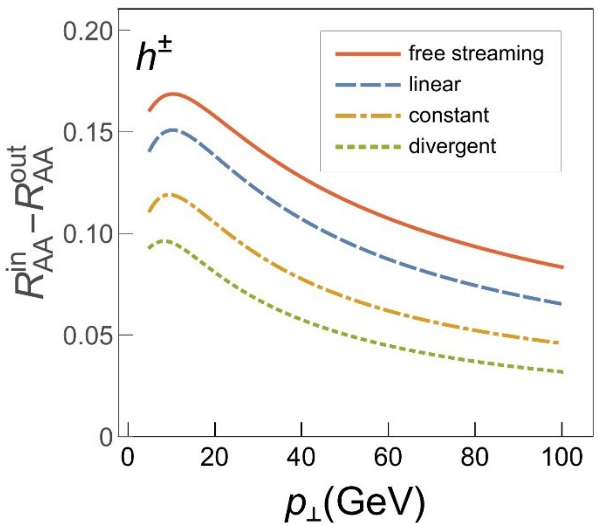

The same curve ordering as modified T profiles in $(\overline{L}_{in}, \overline{L}_{out})$ region.

v_2 differences originate from interactions of high-p⊥ parton with *thermalized* QGP, and *not the initial stages*!